Available online at www.sciencedirect.com
SCIENCE DIRECT®
Journal of Nuclear Materials 329–333 (2004) 477–480
journal of nuclear materials
www.elsevier.com/locate/jnucmat

Dynamic and static hydrogen effects on mechanical properties in pure vanadium

Y. Wang [a,*], M. Kanedome [a], T. Yasuda [a], T. Suda [a], S. Watanabe [a], S. Ohnuki [a], T. Nagasaka [b], T. Muroga [b]

[a] Department of Material Science, Faculty of Engineering, Hokkaido University N-13, W-8, Kita-ku, Sapporo 060-8628, Japan
[b] National Institute of Fusion Science, Toki, Gifu 509-5292, Japan

Abstract

To clarify hydrogen effects on mechanical properties of pure vanadium, two kinds of tensile tests were performed using hydrogen charged miniature specimens at room temperature. One is with hydrogen charging prior to testing, and the other is with hydrogen charging during testing with continuous or intermittent methods. The cathodic hydrogen charging was carried out electrolytically in various concentrations of H_2SO_4 with different current densities. The hydrogen charged specimens were tested to obtain stress–strain curves. The fractography was performed by SEM, and hydride formation and microstructural change were examined by TEM. Hydrogen-induced softening and hardening in vanadium resulted from hydrogen charging. The variations in mechanical property of specimens depended on the amount of dissolved hydrogen, that was determined by hydrogen diffusion and hydrogen desorption. Dislocation motion also plays a role in the variation of flow stress.

1. Introduction

Vanadium-based alloys are candidate structural materials of the first wall and tritium blanket for fusion reactors because of their excellent mechanical properties at elevated temperatures and low induced radioactivity after neutron irradiation. However there are still some critical issues for their engineering use. A major concern is their high affinity with hydrogen and large diffusivity of hydrogen, which, in any of its isotopic forms, can lead to embrittlement at low temperatures. Moreover, the presence of oxygen impurity can generate a synergistic effect on embrittlement [1]. In addition to the static hydrogen effects, several models dealing with hydrogen transport accelerated by mobile dislocations [2] and local supersaturations, or hydrogen effects on the dislocation mobility [3] have been developed. More recently, hydrogen deformation interactions have been shown to strongly control the mechanisms of hydrogen embrittlement for numerous metals and alloys [4]. Owing to its high solubility and large diffusivity in vanadium, hydrogen can be more easily accumulated and then result in microstructural changes that influence the mechanical properties resulting in microstructural changes in vanadium. However, experimental studies focused on the dynamic hydrogen effects in vanadium are very scarce. In contrast to the main studies related to the alloys, the static and dynamic hydrogen effects on the mechanical properties of pure vanadium are evaluated in this paper as a preliminary experiment in order to understand the basis of the phenomena mentioned above.

2. Experimental procedures

The specimens of pure vanadium (Heat V-L142462) used in this investigation were provided by NIFS.

* Corresponding author. Tel.: +81-11 706 6771; fax: +81-11 706 6772.
E-mail address: wang@loam-ms.eng.hokudai.ac.jp (Y. Wang).

0022-3115/$ - see front matter © 2004 Elsevier B.V. All rights reserved.
doi:10.1016/j.jnucmat.2004.04.087

Chemical composition of this vanadium is given in Table 1 [5]. The specimens were cold-rolled to a thickness of 0.25 mm with 97.5% reduction, were annealed at 900 °C for 1 h. The grain size was about 50 μm on average. Hydrogen charging and tensile testing were carried out at room temperature. Hydrogen charging was conducted by two methods. The static hydrogen charging prior to testing was performed in 1.0 N H_2SO_4 solution with a cathodic current density of 6.7 mA/cm^2. The illustration of the equipment for the dynamic hydrogen charging is shown in Fig. 1. The dynamic hydrogen charging started as soon as yielding occurred during tensile testing. In the intermittent method, the hydrogen charging was carried out every 5% strain, the duration of each charging step was 5 s. In the continuous method, the hydrogen charging was continued until failure. In order to change the amount of dissolved hydrogen in specimens, the dynamic charging was curried out in various H_2SO_4 solutions as 0.05 and 1.00 N, and using various cathodic current densities of 6.7, 20.0 and 33.3 mA/cm^2. A graphite anodic electrode was used. Fractography was carried out using a scanning electron microscope (FE-SEM). In order to investigate the dependence of microstructure on the hydrogen charging time, hydride formation and microstructural change were examined using a transmission electron microscope (JEM-2010) operated at 200 kV. The samples used for TEM observation were cut from the miniature specimens after tensile testing (Fig. 1). Mechanical properties of the specimens were determined by tensile testing at a strain rate of 6.7×10^{-4} s^{-1} on an Instron type tensile machine.

Table 1
Chemical composition of heat V-L142462

Elements	Concentration
Cr	0.0002 (wt%)
Ti	0.0006 (wt%)
O	120 (wt ppm)
C	116 (wt ppm)
N	69 (wt ppm)

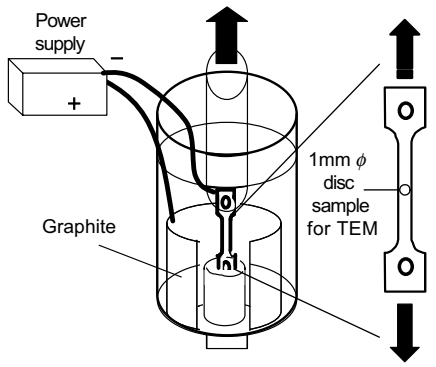

Fig. 1. Charging cell and specimen for the dynamic hydrogen charging.

3. Results

3.1. Static effect

The relationships between yield strength (YS), ultimate tensile strength (UTS) and the duration of hydrogen pre-charging were given in Fig. 2. The YS and UTS decreased initially with charging time and turned to increase from the minimum point at about 30 s. The YS and UTS tended to increase very slowly above 120 s. The initial softening suggests enhancement on the dislocation mobility by dissolved hydrogen, whereas the following hardening indicates the effect of solid-solution hardening by hydrogen at static hydrogenated conditions. As can be seen from Fig. 3, the approximate ductile fracture for 60 s charging and the brittle cleavage fracture for 120 s charging were confirmed. Hydride formation was confirmed after charging for 120 s, as shown in Fig. 4.

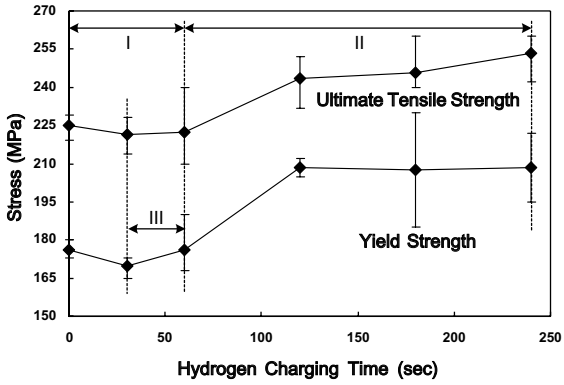

Fig. 2. YS and UTS in V after static hydrogen charging at room temperature.

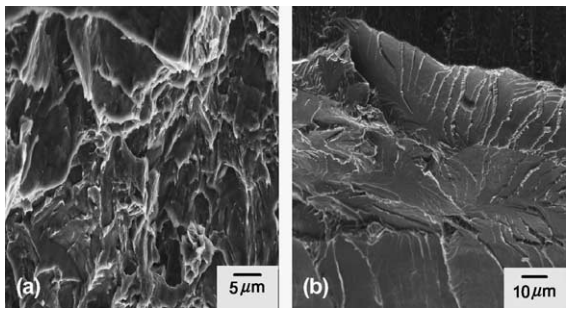

Fig. 3. SEM fractographs after static charging, (a) ductile fracture for 60 s charging and (b) cleavage fracture for 120 s charging.

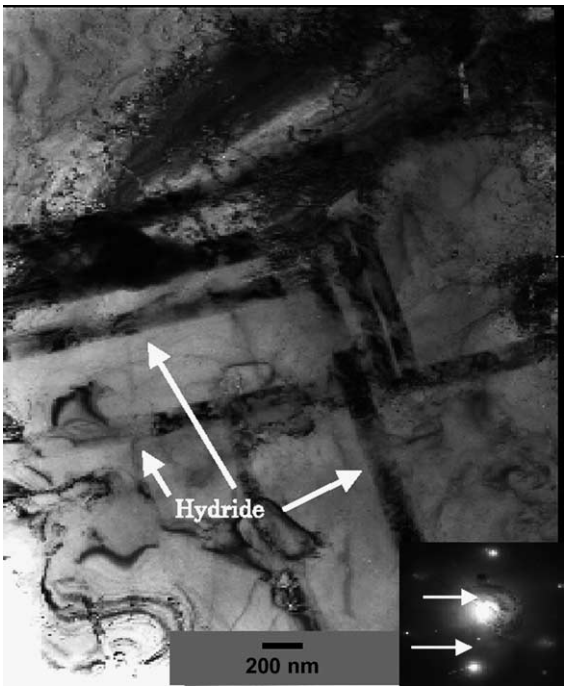

Fig. 4. Hydrides and dislocations in V after static charging for 120 s.

3.2. Dynamic effect

The stress–strain curves for tensile testing with dynamic intermittent-charging in low and high hydrogen charging are shown in Figs. 5 and 6, respectively. The flow stress abruptly decreased at the start of hydrogen charging, and then the serrations occurred during charging. Sharp recovery of the flow stress was initiated soon after charging stopped. The recovered stress can exceed the former flow stress in high hydrogen charging (Fig. 6).

As shown in Figs. 7 and 8, there is no significant difference in the behavior of flow stress soon after

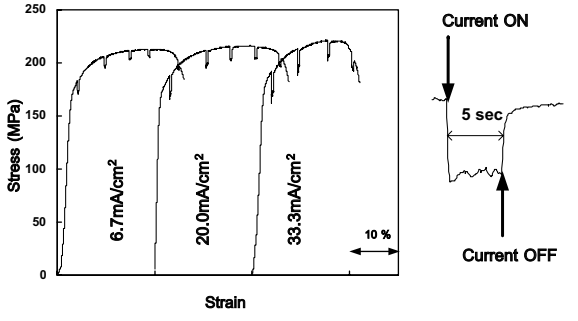

Fig. 5. Stress–strain curves for intermittent dynamic charging in 0.05 N H_2SO_4 solution.

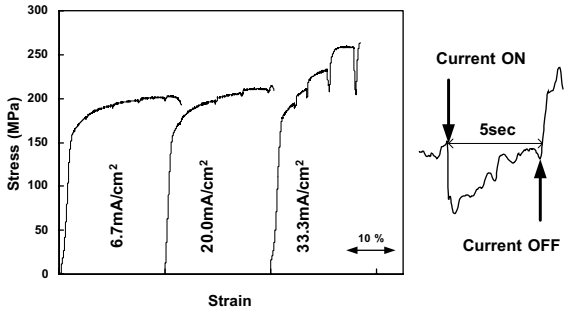

Fig. 6. Stress–strain curves for intermittent dynamic charging in 1.0 N H_2SO_4 solution.

starting charging between the intermittent and the continuous method. Afterward, the plastic deformation continued under lower stress until failure in lower hydrogen charging (Fig. 7). However, in higher hydrogen charging, the flow stress continually increased after an instantaneous recovery until failure due to hydrogen embrittlement (Fig. 8).

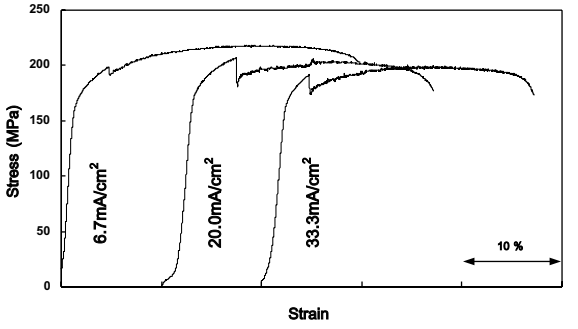

Fig. 7. Stress–strain curves for continuous dynamic charging in 0.05 N H_2SO_4 solution.

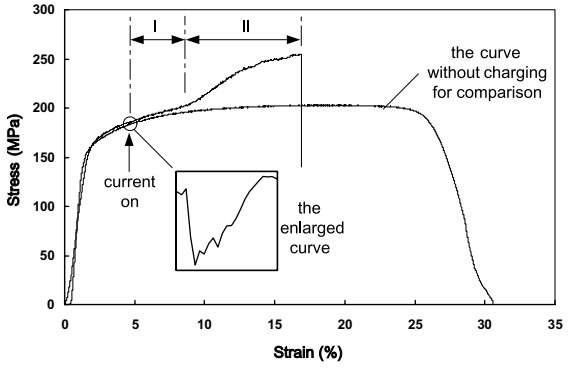

Fig. 8. Stress–strain curve for continuous dynamic charging in 1.0 N H_2SO_4 solution at 6.7 mA/cm^2.

4. Discussion

It is well known that the diffusivity of hydrogen in metals is the fastest among that of any atom in a solid. The diffusion coefficient of hydrogen in vanadium is 3.1×10^{-4} $cm^2\,s^{-1}$ at room temperature [6]. In experimental results, the response time of flow stress drop on hydrogen charging was very short, about 0.5–1.0 s.

All experimental results can be explained as the effects of hydrogen diffusion and hydrogen desorption on dissolved hydrogen in vanadium. Because the grain boundaries are the most favored sites for hydrogen accumulation, much hydrogen is presumably accumulated at grain boundaries in the case of low hydrogen charging. Therefore, for the drop of flow stress, it is a reasonable assumption that accumulated hydrogen can reduce Peierls potential and prompt the formation of kink pairs and also improve its velocity [7]. In term of the 'kink pair' theory, screw dislocations play an important role in plastic deformation of vanadium that is a bcc structure. Hydrogen is trapped at lattice imperfections such as vacancies and dislocations with increasing hydrogen concentration. Thus, pinning obstructs dislocation motion and flow stress increase. As, hydrogen diffused into grain can form Cottrell atmospheres, and macroscopic hardening of vanadium occurs. It is known as solid-solution hardening. Furthermore, hydrides that caused hydrogen embrittlement can be formed with high hydrogen concentrations. Fig. 8 shows the competitive effect of hydrogen desorption on hydrogen diffusion in zone I, and indicates a process from solid-solution hardening to hydrides forming in zone II. The elongation is in a sharp contrast to that of the curve without charging, the significant decrease in elongation suggests that hydrogen embrittlement occurred finally. In Fig. 2, softening and hardening occurred in zone I and zone II, respectively. The softening, which occurred up to 30 s in zone I, may be due to prompting dislocation motion in low hydrogen concentration. However, it should be noted that the competition between effects of softening and solution hardening was seen in zone III. As shown in Fig. 2, the existence of critical hydrogen concentration in zone I is suggested, above which the hydrogen diffusion into grains may gradually become significant. The result of Fig. 4 demonstrates that the hardening above 120 s in Fig. 2 coincided well with hydrides forming. On the other hand, the plastic deformation of specimens can prompt hydrogen desorption [8,9] that affects hydrogen concentration or local hydrogen concentrations contrary to predictions of hydrogen diffusion. Hydrogen desorption presumably results in the recovery of flow stress soon after stopping hydrogen charging. The serration of flow stress during dynamic hydrogen charging can be explained by the competing effects of hydrogen diffusion and hydrogen desorption. So far, various experimental results are attributed to the effect of the competition between hydrogen diffusion and desorption in vanadium.

5. Conclusion

Static hydrogen charging effects: hydrogen charging prior to tensile testing generally resulted in hydrogen-induced hardening shown in yield strength and ultimate tensile strength. In such case, hydride structures were formed inside the specimens. However, hydrogen-induced softening was observed for low hydrogen charging.

Dynamic hydrogen charging effects: an obvious drop in flow stress developed right at the start of the dynamic hydrogen charging; where the response time was of order 0.1 s. With an increase in the charging current density or the electrolyte concentration, the hydrogen-induced softening transitions to hardening. Those results suggest that hydrogen-induced phenomena can be attributed to extensive large diffusivity under deformation and the enhanced dislocation motion, as well as dislocation pinning due to hydrides forming in high charging.

References

[1] J. Chen, S. Qiu, et al., J. Nucl. Mater. 302 (2002) 135.
[2] J.K. Tien, S.V. Nair, et al., Metall. Trans. 7A (1976) 821.
[3] J.P. Hirth, Metall Trans. 11A (1980) 861.
[4] J. Chêne, A.M. Brass, Mater. Sci. Eng. 242 (1998) 210.
[5] Nagasaka et al., in private communication.
[6] U. Freudenberg, J. Völkl, et al., Scr. Metall. 12 (1978) 165.
[7] H. Matsui, H. Kimura, S. Moriya, Mater. Sci. Eng. 40 (1979) 207.
[8] M. Nagumo, K. Takai, et al., J. Alloys Comp. 293–295 (1999) 310.
[9] T. Nishiue, Y. Kaneno, H. Inoue, T. Takasugi, Intermetallics 11 (2003) 817.